Neutral beam injection at ASDEX Upgrade: transmission and beamline losses

N. den Harder, D. Rittich, G. Orozco, C. Hopf, and the ASDEX Upgrade Team

Max-Planck-Institut für Plasmaphysik, Boltzmannstraße 2, D-85748 Garching, Germany

Introduction

Neutral Beam Injection is the main heating system at the ASDEX Upgrade tokamak. With 20 megawatts it represents over half of the installed heating power[1]. For an accurate characterization of the NBI heating and current drive profiles it is necessary to know the beam properties. These properties also determine losses in the duct, through geometrical scraping and reionization, which have led to melt damage of vacuum components in the past. In the current contribution, beam characteristics are determined with beam emission spectroscopy in combination with ion-optics calculations. These characteristics are used as input values for a code which calculates power loads on duct components and the geometrical transmission of the duct.

Experimental geometry

At the ASDEX Upgrade tokamak, the installed NBI power is 20 megawatts in deuterium, equally distributed over two beam boxes. In both beam boxes, the 4 NBI sources are arranged in a rectangle, with a nominal beam power of 2.5 MW each. In beam box 1, ions are accelerated from an arc plasma over a potential drop of 60 kV. The sources in this box inject fairly normal to the plasma, with tangency radii of 0.53 and 0.93 meters. Beam box 2 operates at an extraction voltage of 93 kV, with RF-sources. The sources in this box inject more tangentially, with tangency radii of 0.84 and 1.29 meters. The sources with the largest tangency radius are vertically steerable over an angular range of $\pm 0.5°$.

In each NBI source, D^+, D_2^+, and D_3^+ ions are extracted from a plasma by means of 3 grids[2]. In each source, the two grid halves are tilted vertically by 0.87° to focus the beam halves. In addition, the holes in the first grid are offset to induce an inward steering of the outer beamlets. Directly after the source the extracted positive ions interact with background gas in a tapered pipe, leading to dissociation of the molecular ions and neutralization. In addition, background gas interaction leads to excitation and light emission. The Balmer-α line, with an average air wavelength of 656.093 nm for deuterium, is used to diagnose the beam[5]. The emission spectrum is collected along a vertical line of sight with an angle of 50° to the source normal, at 1.5 meters distance from the source.

Computational method

The NBI power density is calculated as a sum of Gaussian beamlets. The beamlets are parametrized by the divergence ε, which is half the opening angle of a cone with power densities that are $1/e$ of the on-axis power density. The normalized power density for a single beamlet as function of parallel ($l_\parallel$) and perpendicular ($l_\perp$) distance with respect to the beamlet axis is

$$F\left(l_\parallel, l_\perp\right) = \frac{1}{2\pi\sigma_{l_\perp}^2} \exp\left(-\frac{l_\perp^2}{2\sigma_{l_\perp}^2}\right), \qquad \text{where} \qquad \sigma_{l_\perp} = \frac{l_\parallel \tan(\varepsilon)}{\sqrt{2}}. \tag{1}$$

The beamlet starting locations are taken from design specifications. The beamlets starting direction is perpendicular to the grids, with a deflection angle due to the beamlet offset steering, parametrized by a steering factor δ which has the units of degrees of steering per mm offset. Complete NBI sources can be rotated around a ball joint as installed in the experiment.

The Doppler shift of the beam emission depends on the angle between vector $\vec{r}_{ij}$ from beamlet i to observation volume j, and the spectroscopic Line Of Sight $\vec{e}_{\mathrm{LOS}}$:

$$\lambda = \lambda_0 \left(1 - \frac{v}{c}\right) \frac{\vec{r}_{ij} \cdot \vec{e}_{\mathrm{LOS}}}{|\vec{r}_{ij}||\vec{e}_{\mathrm{LOS}}|} \tag{2}$$

where v is the speed of the emitter, c is the speed of light, and λ_0 is the wavelength of the emission line. It is assumed that the viewing system is perfectly collimated, i.e. that $\vec{e}_{LOS}$ is identical for all the observation volumes. To calculate beam emission spectra, the wavelength and power density is calculated for each beamlet at a collection of points in the observation volume. The spectrum is the histogram of all these wavelengths, weighted by the power density. Spectra are calculated for the three energy components, and convolved with the instrument function of the spectrometer.

Geometry data of components around the NBI beam line is read from STL files, which describe surfaces as collection of triangles. Power loads on surfaces are calculated by projecting the contribution of each beamlet onto the surface normal. Shadowing by beamline components is implemented with the modified BSP tree algorithm, available in the Visualisation Toolkit[4].

Results

Beam parameters are determined with emission spectra. In Figure 1a, the main energy component of the spectrum is shown, which is taken under standard conditions for box 2, i.e. an acceleration potential of 93 kV. The spectra have a double peak structure because the two grid halve normals intersect with the viewing line of sight at different angles. The synthetic spectra are calculated as function of two input parameters, the beamlet steering factor δ describing the beamlet offset steering, and the divergence ε.

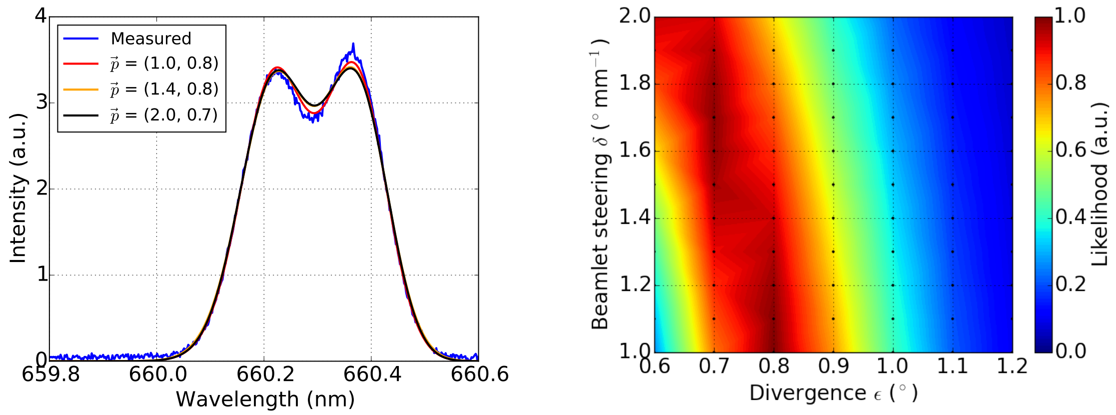

(a) Fits with input parameters $\vec{p} = (\delta, \varepsilon)$ (b) Likelihood for Gaussian fits

Figure 1: Different input parameters (δ [° mm^{-1}], ε [°]) result in equally good fits. At a δ of 1.44° per mm, the best divergence ε is $0.76^{+0.18}_{-0.14}$ degrees for the E_1 component.

The likelihood of the fits was determined based on the Gaussian noise in the measurements and the difference between measurement and model. Figure 1b shows the scaled distribution. Several parameter combinations are equally likely. As additional constraint, the beamlet steering factor was determined with IBSimu ion optics calculations[3]. With the calculated beamlet steering of 1.44° per mm, the divergence of the full energy component is $0.76^{+0.18}_{-0.14}$ degrees. The half and third energy components have similar divergences.

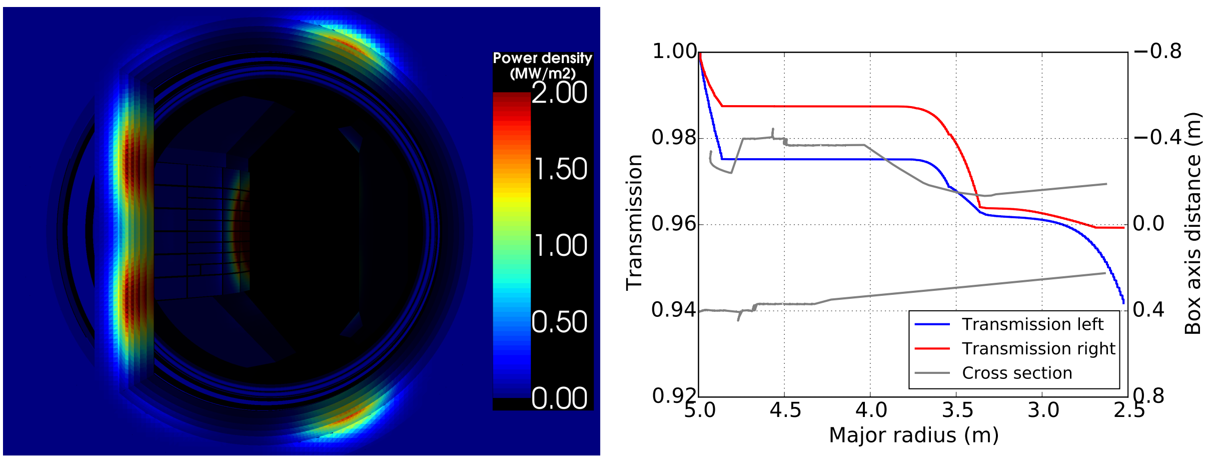

(a) Power load on box 2 duct components (b) Transmission and cross section of duct

Figure 2: Taking into account shadowing, the power load on the full 3D geometry, and the transmission is calculated. Results shown for a divergence of 0.8°.

With the beamlet parameters, the power density on the duct components is calculated. Figure 2a shows the power loads in the duct of box 2 seen in the beam direction, when all four sources are in use. Most of the energy is deposited on the box exit scraper (D-shaped component in front), and the A-Port shield (tile segments at the left side in beam direction). Both parts are designed to handle a large heat load. With the deposited power, the geometrical transmission is calculated for the sources individually, as shown in Figure 2b. The transmission is usually assumed to be lower due to a non-Gaussian part of the beamlet power distribution, but this is difficult to argue since the emission spectra do not show much intensity at the wings. Although the box 2 exit scraper is more restrictive at the left side in beam direction, the transmission of the sources at the left and the right of the box are similar. Analysis of the shadowing calculation shows that the regions with melt damage in the previous campaign are shielded by the scraper, confirming the hypothesis that the damage is caused by reionized particles deflected by the magnetic field. An improved symmetrical scraper has been installed since the start of the 2017 ASDEX Upgrade campaign.

Outlook

A code was developed to calculate beam emission spectra, power loads on components, and duct transmission for the neutral beam injection system at ASDEX Upgrade. At this stage, reionization and the influence of the magnetic field is neglected. The flanges which have shown melt damage in previous campaigns are shielded by the box exit scraper, confirming the hypothesis that the damage is caused by reionized particles deflected by the magnetic field. Gas flow and magnetic field calculations are in progress to determine the background gas density in the NBI box and the magnetic field distribution. These values will be used as input for further simulations in which individual particles will be iterated through the prescribed magnetic field, where the background gas interaction is taken into account with a Monte Carlo scheme. The resulting power density distributions will be used to determine the limits of the operational parameter space.

References

[1] B. Streibl *et al.*, Fusion Science and Technology **44**, 578-592 (2003)

[2] P. Franzen *et al.*, Fusion Engineering and Design **56-57**, 487-491 (2001)

[3] T. Kalvas *et al.*, Review of Scientific Instruments **81**, 02B703 (2010)

[4] W. Schroeder *et al.*, *VTK: An Object-Oriented Approach to 3D Graphics*, 4th edition, (Kitware, 2006)

[5] W. L. Wiese and J. R. Fuhr, Journal of Physical and Chemical Reference Data, **3**, 565-720 (2009)

This work has been carried out within the framework of the EUROfusion Consortium and has received funding from the Euratom research and training programme 2014-2018 under grant agreement no. 633053. The views and opinions expressed herein do not necessarily reflect those of the European Commission.